

Gaussian beam optimization for O–X mode conversion

A. Cappa¹, E. Holzhauser², F. Castejón¹, M. Tereshchenko³, A. Fernández¹ and A. Köhn²

¹ *Laboratorio Nacional de Fusión–CIEMAT, Madrid, Spain*

² *Institut für Plasmaforschung, Universität Stuttgart, Stuttgart, Germany*

³ *Russian Academy of Sciences, General Physics Institute, Moscow, Russia*

Introduction

As it is well-known, the excitation of electron Bernstein waves (EBW) by means of the O–X–B mode conversion technique needs a very precise parallel refraction index (n_{\parallel}) at the O–mode cutoff layer [1]. In order to achieve the maximum conversion efficiency, the launched wave must reach its cutoff with $n_{\parallel}^{opt} = \sqrt{u/(1+u)}$ and $n_{\perp}^{opt} = 0$, where $u \equiv \omega_c/\omega$ is the local normalized cyclotron frequency. In the frame of the WKB theory, where the homogeneous plasma dispersion relation is used, this result describes the behaviour of a single plane wave, which differs strongly from the highly focused Gaussian beams used in conventional ECR heating applications. The conversion efficiency behaviour of an arbitrary Gaussian beam was studied in the TJ–II stellarator [2] using two different ways of representing a beam with rays. The first approximation considers rays distributed perpendicularly to the wave front surface whereas the second one takes into account the plane waves spectrum of the beam (Fig. 1). From these studies, an optimum beam was derived. The aim of the present contribution is to clarify the ray tracing results by using two–dimensional full wave calculations in a cylindrical geometry.

Ray tracing calculations (3–D)

In the two approximations mentioned above, the total O–X conversion efficiency of the Gaussian beam is calculated using the ray tracing code TRUBA [3] where the single ray transmission efficiency η is obtained with the one–dimensional O–

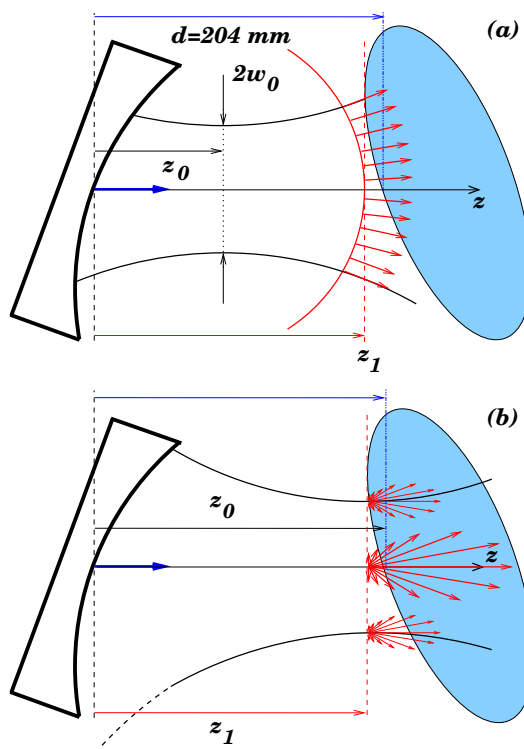


Figure 1: *Schematic beam representation. (a) Perpendicular rays distribution for any z_0 and (b) plane wave spectrum distribution used for $z_0 = 0.2$ m.*

mode tunneling theory [4]. For a given frequency ω , it can be shown that

$$\eta = \exp\left(-\pi \frac{\omega}{c} \frac{n_e}{|\nabla n_e|} \left(\frac{u}{2}\right)^{1/2} \left[n_{\perp}^2 + 2(1+u)(n_{\parallel} - n_{\parallel}^{opt})^2\right]\right) \quad (1)$$

The total beam conversion efficiency is given by $T \equiv \sum_1^{N_r} \eta_j \rho_j$, where η_j is the single ray efficiency and ρ_j is the ray weight. In the first approximation, the rays are weighted according to the beam power distribution. In relation with the second approximation, we consider the field of a Gaussian beam, which is defined by its frequency, its waist (w_0) and the position of its waist along the propagation direction (z_0), written in terms of a superposition of plane waves, i.e.

$$\mathbf{E}(\mathbf{r}) = \int_{-\infty}^{\infty} dk_x \int_{-\infty}^{\infty} dk_y \mathbf{A}_{\mathbf{k}} e^{ik_z z} e^{ik_x x} e^{ik_y y} \quad (2)$$

with $k_z = \sqrt{k^2 - k_{\perp}^2}$, $k = \omega/c$ and $k_{\perp}^2 \equiv k_x^2 + k_y^2$. The inverse Fourier transform at $z = z_0$ is

$$\mathbf{A}_{\mathbf{k}} e^{ik_z z_0} = \frac{1}{(2\pi)^2} \int_{-\infty}^{\infty} dx \int_{-\infty}^{\infty} dy \mathbf{E}(x, y, z_0) e^{-ik_x x} e^{-ik_y y} \quad (3)$$

Using now $\mathbf{E}(x, y, z_0) = \mathbf{E}_0 e^{-[r^2/w_0^2]}$ and evaluating explicitly the integral in eq. (3), we get

$$\mathbf{A}_{\mathbf{k}} = \frac{\mathbf{E}_0 e^{-ik_z z_0}}{4\pi} w_0^2 e^{-\frac{1}{4} w_0^2 k_{\perp}^2} \quad (4)$$

By adding coherently all the complex amplitudes given by eq. (4), we recover the original beam field distribution. Obviously, this cannot be fully reproduced by ray tracing means since only $|\mathbf{A}_{\mathbf{k}}|^2$ is taken into account in the simulation. Each of the zones represented by one ray in the first approximation (Fig. 1 (a)) is now described with a bunch of rays launched in all directions ($k_z > 0$), weighted according to $|\mathbf{A}_{\mathbf{k}}|^2$ and to the beam power distribution (Fig. 1 (b)). For a given beam waist, the calculations with this approximation have been performed only for $z_0 = 0.2$ m. Figure 2 shows the total beam conversion efficiency obtained with both approaches

for three different values of the beam waist. Different focusing distances have been calculated in the case of perpendicular rays (141 rays have been considered). In principle, in the far field

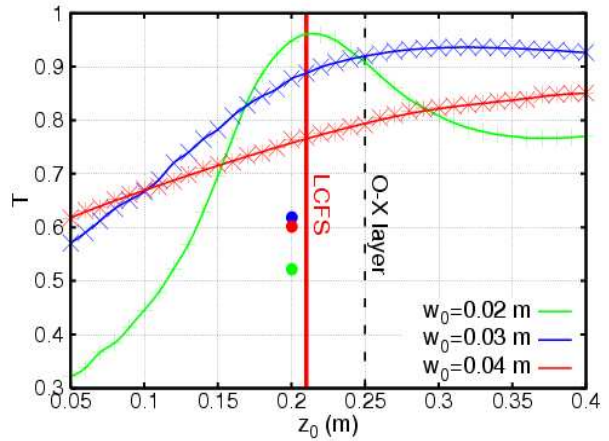


Figure 2: Total conversion efficiency obtained in the TJ-II stellarator ($\omega/2\pi = 28$ GHz) with the perpendicular rays approximation (solid lines) and the \mathbf{k} spectrum approach (dots). The O-X layer and the LCFS location are shown.

region of the beam, defined by $|z - z_0| \gg \pi w_0^2 / \lambda$ (≈ 0.1 for $f = 28$ GHz and $w_0 = 0.02$ m), the main contribution to the field amplitude in a particular direction is given essentially by the plane wave which has its \mathbf{k} along that direction [5]. For these conditions, the approximation seems reasonably valid. However, T appears overestimated when the beam focus is located near the critical surface ($T \approx 0.95$ for $w_0 = 0.02$ m) and the launched rays are taken almost parallel (the wave front is almost plane). In fact, a much lower conversion efficiency is obtained when the plane waves approximation is taken into account ($T \approx 0.52$ for $w_0 = 0.02$ m with 1147 rays). For wider beams, their bigger size spoils the conversion efficiency due to the plasma curvature unless the focus is located beyond the critical surface, where the beam curvature matches the plasma curvature. From these considerations, the most efficient beam seems to be the one with $w_0 = 0.03$ m focused beyond the O–X conversion layer (z_0 is limited by the mirror size).

Full-wave calculations (2–D)

In order to check the previous results, full-wave simulations have been performed in the poloidal and the toroidal planes of a cylindrical plasma (Fig. 3) using the Finite-Difference Time-Domain method [6]. An homogeneous magnetic field corresponding to the TJ-II field encountered at the O–X conversion layer ($B = 0.87$ T), as well as the density profile used in the ray tracing calculations, are being considered in the simulations. The results obtained in the toroidal (or horizontal) plane are represented in Fig. 4 for (a) $w_0 = 0.02$ m and (b) $w_0 = 0.04$ m. The incoming (red) and reflected (blue) beam power are shown. The O-mode cutoff surface ($q \equiv \omega_p^2 / \omega^2 = 1$) and the upper hybrid resonance (UHR) are also shown. According to eq. (4), the beam with smaller w_0 has a wider spectrum and therefore a lower conversion efficiency ($T = 65\%$) in respect to the wider one ($T = 86\%$). In this case, where no plasma curvature effects are included, the efficiency increases as the beam gets wider. Compared to these results, the calculations in the poloidal (or vertical) plane (Fig. 4 (c) and (d)) show that T is reduced due to the plasma curvature. The reduction is stronger for wide beams, which see a larger plasma zone. However, the difference between (c) and (d) is not so large due to the combination of the curvature and spectrum effects. Finally, the dependence of T on the matching parameter R_c (plasma curvature radius over beam curvature radius evaluated near

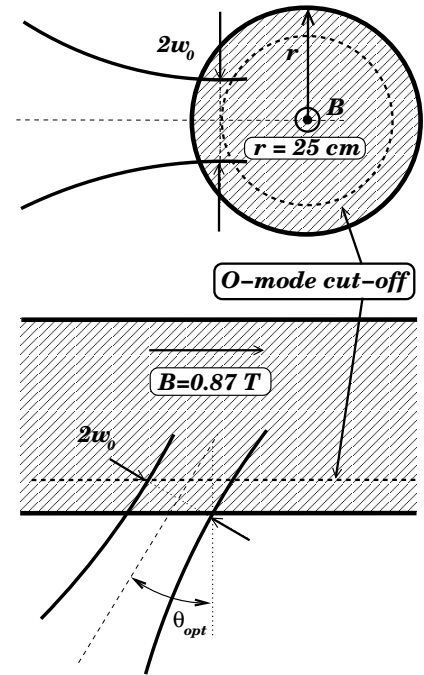


Figure 3: Cylindrical plasma used in the 2–D full wave calculations. $R_p \equiv r = 25$ cm.

the O–X layer) is represented in Fig. 5. It is seen that in the poloidal plane the conversion efficiency is sensitive to the deviations from the perfect matching condition ($R_c = 1$). For beams with smaller waist, the efficiency decreases but also the matching errors are less important.

Conclusions

Different ways of representing a Gaussian beam with ray tracing have been tested. In the limited set of parameter space studied, the results suggest that the best beam is the one with $w_0 = 0.03$ m focused beyond the O–X conversion layer. The comparison between the ray tracing simulations and the 2–D full-wave solutions, only for the special case where the waist is located close to the LCFS, shows a better agreement with the planes waves approximation while the non–validity of the perpendicular rays approximation is also demonstrated in this case. A full–wave 3–D reconstruction from the 2–D results, that will allow us to compare similar situations, is in progress. Finally, the full–wave simulations in the vertical plane have shown that the optimum T is achieved if $R_c \approx 1$.

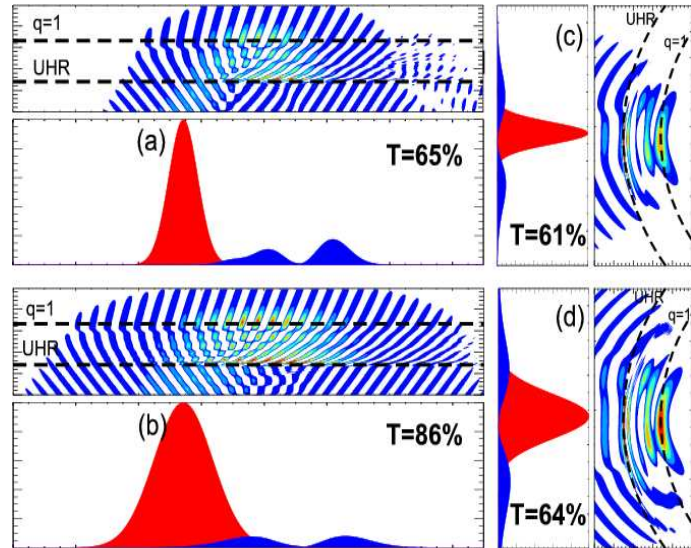


Figure 4: Full–wave calculations in the horizontal (left) and vertical (right) planes. The conversion efficiency T is shown in the graphs. The reflected power is due to the unconverted power–fraction from the wings of the angular beam pattern.

References

- [1] J. Preinhaelter and V. Kopecký, J. of Plasma Phys. **10**, (1973) 1.
- [2] A. Cappa et al., 31st EPS Conf., ECA **28 B** (2004).
- [3] M. Tereshchenko et al., 30th EPS Conf., ECA **27 A** (2003).
- [4] E. Mjølhus, J. of Plasma Phys. **31**, (1984) 7.
- [5] D.H. Martin et al., IEEE Trans. on Microwave Theory and Tech. **41**, (1993) 1676.
- [6] A. Taflove, S.C. Hagness, “Computational Electrodynamics: The Finite–Difference Time–Domain Method”, Artech House, (2000).

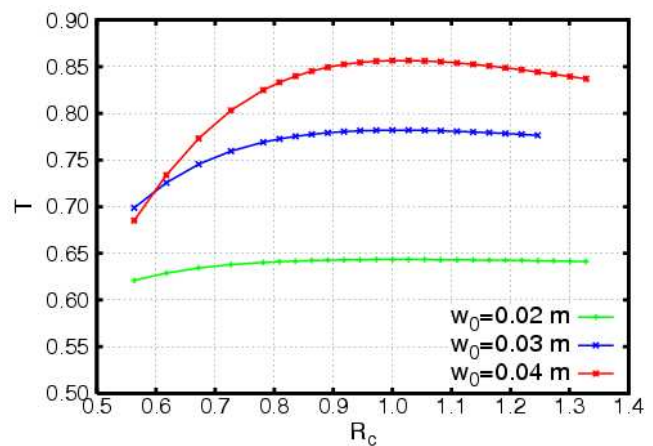


Figure 5: Dependence of T on the matching parameter $R_c \equiv R_p/R_b$, for different beam waists.